Journal of Maps

ISSN: (Print) (Online) Journal homepage: https://www.tandfonline.com/loi/tjom20

The Quaternary landforms of the Büyük Menderes Graben System: the southern Menderes Massif, western Anatolia, Turkey

Emrah Özpolat , Cengiz Yıldırım & Tolga Görüm

To cite this article: Emrah Özpolat , Cengiz Yıldırım & Tolga Görüm (2020) The Quaternary landforms of the Büyük Menderes Graben System: the southern Menderes Massif, western Anatolia, Turkey, Journal of Maps, 16:2, 405-419, DOI: 10.1080/17445647.2020.1764874

To link to this article: https://doi.org/10.1080/17445647.2020.1764874

JOURNAL OF MAPS
2020, VOL. 16, NO. 2, 405–419
https://doi.org/10.1080/17445647.2020.1764874

Taylor & Francis
Taylor & Francis Group

Science

The Quaternary landforms of the Büyük Menderes Graben System: the southern Menderes Massif, western Anatolia, Turkey

Emrah Özpolat [a,b], Cengiz Yıldırım [a] and Tolga Görüm [a]

[a]Eurasia Institute of Earth Sciences, Istanbul Technical University, Istanbul, Turkey; [b]Department of Marine, Earth, and Atmospheric Sciences, North Carolina State University, Raleigh, NC, USA

ABSTRACT

We present the first detailed Quaternary landform map of the Büyük Menderes Graben System, located in western Turkey which is one of the most active extensional domains in the world. The main map was produced with a combination of TanDEM-X (12.5 m resolution), Red Relief Image Map, unmanned aerial vehicle, Google Earth images, and multiple fieldworks. The main map is presented at a scale of 1:160,000 although landforms were mapped at a scale of 1:15,000. The ten Quaternary landforms were defined considering their surface morphology and depositional environment. The alluvial fans, river terraces, and floodplains are the most common landforms. The spatial pattern of the alluvial fans and river terraces showed the variable rates of tectonics and surface processes along the strike of the graben system. The distribution of the meander cut-offs and paleo-shorelines imply that Büyük Menderes Graben System is vulnerable to geohazards like flash-flood sedimentation and flood events.

ARTICLE HISTORY
Received 3 March 2020
Revised 30 April 2020
Accepted 1 May 2020

KEYWORDS
Extensional landscape; alluvial fan; river terrace; Red Relief Image Map; western Anatolia; Menderes Massif

1. Introduction

The Quaternary landforms of dynamic extensional regions such as western Anatolia (Turkey) (Dewey & Şengör, 1979), Basin and Range (USA) (Blair, 1999; Leeder & Mack, 2001), Central Greece (Fountoulis et al., 2015; Tsodoulos et al., 2008), and Apennines (Italy) (Bertotti et al., 1997; Valente et al., 2019) in terms of active tectonics and sedimentation can be used to help to understand the evolution of these landscapes. The western Anatolian Extensional Province (WAEP) is one of the rapidly extending regions and dynamic landscapes on Earth (Reilinger et al., 2006). WEAP is part of a zone of distributed extensional deformation affecting a large area (the Aegean extensional province) that includes the Aegean Sea, Greece, Macedonia, Bulgaria and Albania, and is bounded by the Hellenic Trench in the south (Bozkurt, 2000) (Figure 1). Back-arc extension as a result of the southward retreat of the Hellenic Trench is the driving force defining neotectonic processes in the region (Barka & Reilinger, 1997; Dewey & Şengör, 1979). This rapid extension at a rate of ~20 mm/yr (Aktug et al., 2009) is accommodated by several normal and detachment faults that form horst-graben systems. The Menderes Massif is located at the center of this tectonic deformation where pervasive crustal extension in the Quaternary led to the development of extensional grabens delimited by faults trending E-W, NW–SE, and NE–SW (Bozkurt, 2000; Gürer et al., 2009; Kazanci et al., 2009; Ocakoğlu et al., 2014).

The Büyük Menderes Graben System (BMGS) bounded by active normal faults is one of the most active depositional settings of western Anatolia (Altunel, 1998; Sümer et al., 2013). The drainage network of the graben transport sediments from hundred-kilometers inner parts of western Anatolia and the rapidly uplifted Menderes Massif surround the graben (Ergin et al., 2007). The rapid erosion rate (Gessner et al., 2013; Wölfler et al., 2017) on the Menderes Massif gives rise to high sedimentation rates and formation of depositional landforms along the BMGS. The stratigraphy and morphology of depositional landforms are useful to understand the source to sink relationships in this kind of dynamic setting. Also, well-preserved landforms such as relict and modern alluvial fans, river terraces, and floodplains deformed by normal and detachment faults provide excellent exposures to understand the Quaternary landscape evolution of the region.

Historical and paleo-seismological records reveal intensive seismic activity with records of many destructive earthquakes along the BMGS (Mozafari, 2019; Yönlü et al., 2010). Archeological data also reveal that earthquakes were not the only geohazards for major ancient cities such as Miletus, Myous, and Priene built within the graben. They also struggled with rapid alluvial sedimentation that gave rise to infilling at harbors

CONTACT Emrah Özpolat ozpolat16@itu.edu.tr, eozpola@ncsu.edu Eurasia Institute of Earth Sciences, Istanbul Technical University, Sarıyer- Istanbul, 34469, Turkey

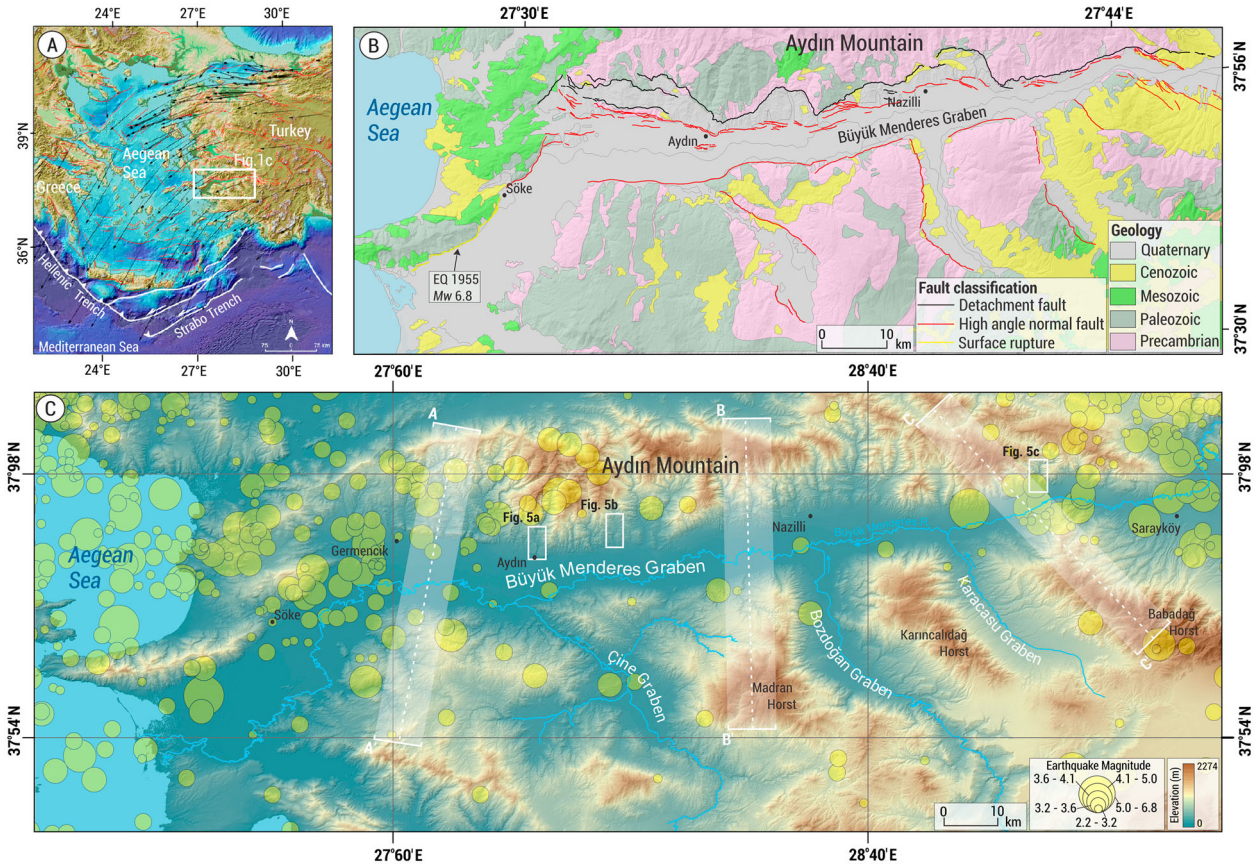

Figure 1. (a) Simplified active tectonic map of the Aegean Sea and the western Anatolia. The white box indicates the study area. The black arrows show the movement direction of the western Anatolia. GPS vectors are from Aktuğ et al. (2009). (b) Geological map of the Aydın Mountain and its near vicinity (compiled from Gürer et al., 2009; Kazanci et al., 2009; Konak & Şenel, 2002). Faults are from Emre et al. (2018). (c) The grabens in the study area. Yellow circles show earthquake epicenters between 1900 and 2019 recorded by the USGS. White boxes show river terraces in Figure 5. Transparent white boxes indicate swath profiles in Figure 7.

and associated loss of wealth (Brückner, 1997; Anthony et al., 2014) (main map 1). Similar events occur even today within the graben. Heavy rainstorms in spring make the alluvial fans and flat river courses in the BMGS is vulnerable to geohazards like flash-flood sedimentation. These events form many meander cut-offs and abandoned river courses affecting agriculture or settlements on the floodplain of the BMGS (Brückner et al., 2017). Although there is a high rate of active faulting and a high rate of sedimentation and geohazards like flooding, the maps associated with the Quaternary geology and geomorphology of landforms along the BMGS are very limited and lack region-wide correlations.

The overarching goal of this study is to provide insights into the evolution of the landscape, especially during the Quaternary. Building a morphostratigraphy of Quaternary landforms is one of the important components of understanding the evolution of the landscape. Therefore, we provided a high-resolution map of Quaternary landforms, and a region-wide morphostratigraphy exposed in different sectors (e.g. Karacasu, Bozdoğan, Çine) of the Büyük Menderes Graben System. Our geomorphic mapping of Quaternary landforms like meander cut-offs and abandoned river courses may provide key information for many of the management practices in terms of geohazards in the study area.

2. Regional setting

The Büyük Menderes Graben, Çine, Bozdoğan, and Karacasu grabens and their mountain-front that form the main subject of this study are considered as the Büyük Menderes Graben System (BMGS). The BMGS covers nearly 2200 km^2 and extends nearly 140 km from the Aegean Sea to Denizli Graben in the east (Figure 1). The Büyük Menderes River (BMR) is the trunk river that transports sediments from inner western Anatolian basins to the Aegean Sea and acts as a local base-level for its tributaries sourced from Aydın Mountain and upstreams of Çine, Bozdoğan and Karacasu Grabens.

The escape tectonics of the Anatolian microplate to Eurasia is a result of the Arabian collision in the east and slab retreat along the Hellenic trench in the west (Armijo et al., 1999; Şengör & Yilmaz, 1981). The back-arc extension as a result of the southward retreat of the slab is the driving force of

neotectonic deformation in western Anatolia (Barka & Reilinger, 1997; Dewey & Şengör, 1979). This extension is taken up largely on E-W and NW-SE trending grabens that dissect the Menderes Massif Core Complex (MMCC) which has been exhumed along the low angle detachment faults. The Büyük Menderes Detachment Fault (BMDF) represents the geological boundary between metamorphic rocks and Plio-Quaternary sedimentary units along the southern flank of the Aydın Mountain (Bozkurt, 2000). The transition from low-angle detachment faulting to high-angle normal faulting occurred in the latest Pliocene to early Quaternary (Oner & Dilek, 2011). The Büyük Menderes Graben has been a depositional center for thick sedimentary layers with the activity of the BMDF since the late Pliocene (Cohen et al., 1995). The BMDF is cut by the high-angle normal faults along the northern margin of the BMG (Figure 1b). These high-angle normal faults deformed the Quaternary sediments and created distinctive topography such as fault scarps, raised fluvial terraces, alluvial fans.

The temperate climate of the region (rainy-mild winters and dry warm summers) with an average rainfall of 644 mm/yr with mixed vegetation (forest, maqui, olive) cover allows fluvial processes to act as a dominant external driver that shape the landscape of the region.

3. Methods

3.1. Datasets and processing

Boulton and Stokes (2018) showed that the TanDEM-X has the highest effective topographic detail compared to digital elevation models such as SRTM, ASTER, AW3D. We used a TanDEM-X (12.5 m resolution) (DLR, 2016) as a base map for the Quaternary landform map. After mapping in the office environment, Quaternary landforms and sediments were confirmed during fieldwork in 2018 and 2019. Nikon rangefinder and D-GPS were used to survey topographic metrics of river terraces.

3.2. Red relief image map (RRIM)

The Quaternary landforms were mapped using Red Relief Image Map (RRIM) mosaics derived from the TanDEM-X. The main concept of RRIM from DEMs is based on multiplying three landform layers: positive openness, negative openness, and the topographic slope (Chiba et al., 2008). Negative openness represents surface concavity and positive openness is characterized by the convexity of the surface (Yokoyama et al., 2002). Negative openness takes higher values such as valley, inside of crater, and landslides while positive openness represents higher values such as crests and ridges. The primary part of RRIM suggested by Chiba et al. (2008) is the definition of a new parameter calculated from:

$$I = \frac{(O_p - O_n)}{2} \quad (1)$$

where O_p is positive openness and O_n is negative openness. The O_p and O_n are shown schematically for values less than 90 degrees. I is a radial limit of calculation for chosen points on a DEM. The gray-scale image layer defines the RRIM I value index and the topographic slope is the red color layer. These parameters suitably eliminate incident light direction dependencies that occur in shaded relief images and express convexity and concavity at the same time (Chiba et al., 2008). In this visualization method, the fusion of the topographic slope and openness rate creates the RRIM. According to Chiba et al. (2008), that red color has the richest tone for human eyes, especially under computer-oriented color space. It should be stated that RRIM does not include information about the elevation and direction of the slope. Thus, elevation data was used on the RRIM (Figure 2).

3.3. Mapping of the landforms

The surface morphology of Quaternary sediments is seen on RRIM (Figure 3). Firstly, Quaternary landforms were separated into 10 units based on their surface morphology using the RRIM method, and Google Earth™ images. Especially useful landforms for tectonic and climatic inferences like alluvial fans and river terraces were separated into subunits. Alluvial fans were divided morphostratigraphically into two subunits based on features like weathering, slope, texture, shape, and entrenchment. Here, for each graben older alluvial fans were coded as Qaf1, while younger alluvial fans were coded Qaf2. River terraces were morphostratigraphically coded for each basin. The highest river terrace was named as Qrt1, and terraces closer to the modern river were called as Qrt2 and Qrt3. Quaternary landforms in the study area were systematically mapped at a 1:15,000 scale. However, given the difficulties in extracting the different river terrace levels, the working scale was around 1:8000. Finally, the main map was presented with print size 1:160,000 to fit ISO A2. The reference coordinate system used was UTM zone 35 north and WGS84 datum. Also, the main map was presented as two sheets due to the width of the west–east axis (Main map 1 and 2).

4. Quaternary landforms

4.1. Relict alluvial fans (Qraf)

During the Late Pliocene, the Büyük Menderes Detachment Fault (BMDF) developed as a major breakaway

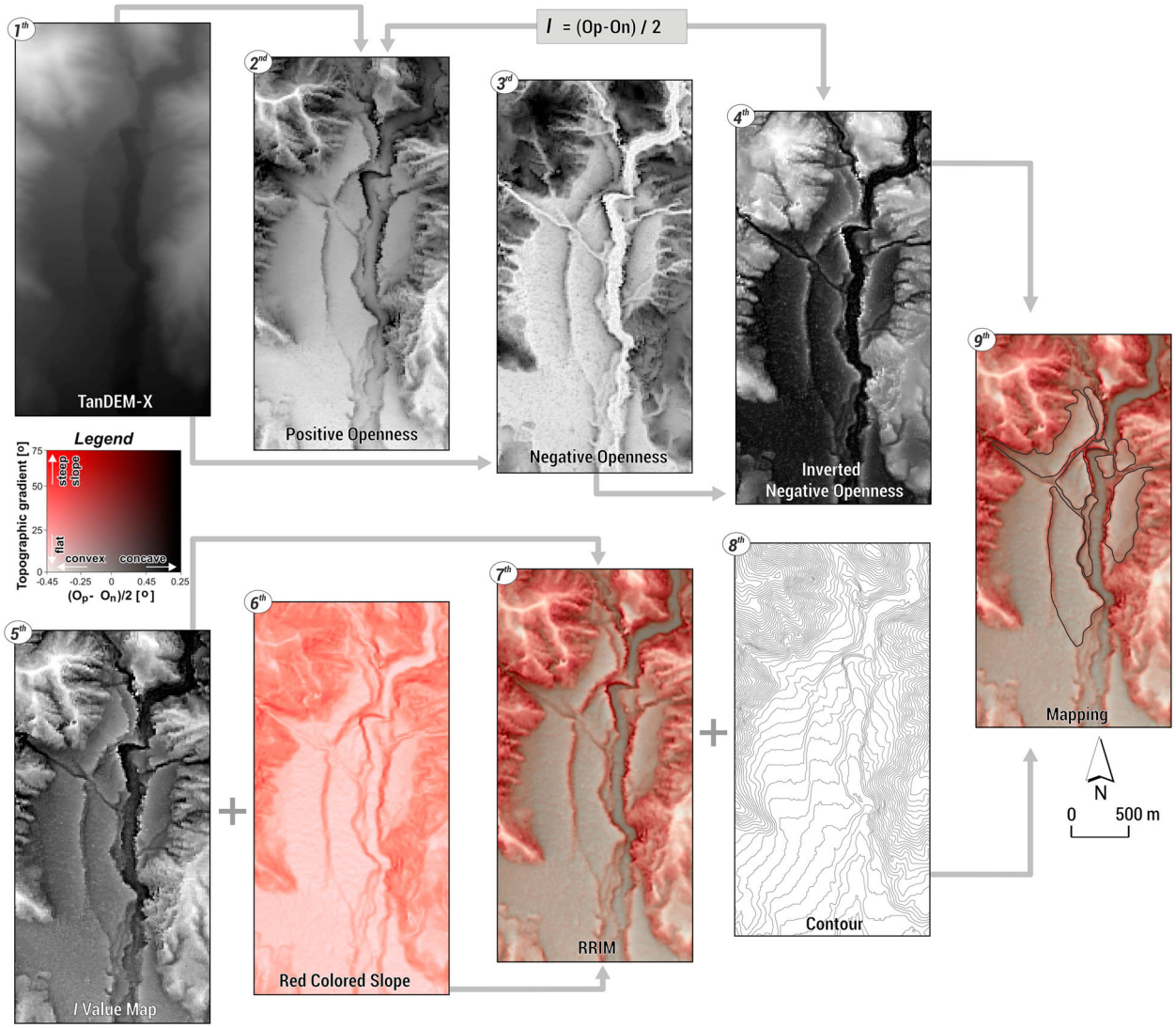

Figure 2. Red Relief Image Map (RRIM) production steps proposed by Chiba et al. (2008). The numbers indicate each processing step for the Esnek river terraces.

detachment fault and its present dip is 30–60° to the south (Gürer et al., 2009). Synchronous with the activity of the detachment fault, terrestrial sediments were deposited along the southern mountain front of the Aydın Mountain. Philippson (1912) called these deposits *Tmolosschutt*. The term '*Tmolosschutt*' was originally used as an ancient name of Bozdağlar in the northern section of the Menderes Massif. However, Philippson (1912) and Erinç (1954) used the term for Plio-Quaternary sediments deposited along the northern flank of Bozdağlar (Mt) and the southern flank of the Aydın Mountain. We termed these sediments relict alluvial fans because they consist of the first alluvial fans deposited along the relict mountain-front of Aydın Mountain (Figure 3d).

Morphologically, these alluvial fan deposits show badlands topography. This morphology can be easily distinguished from other landforms on the RRIM (Figure 3d). The deposits in the western part of the Aydın Mountain, in comparison with the eastern section of the Aydın Mountain have been extensively eroded by rivers (Figure 4a). Along the southern flank of the Aydın Mountain, there is a contrast in the distribution of these deposits. Towards the east of the Aydın Mountain, the widths of these fans become narrow. In the west of the Aydın Mountain, they have an 8 km width in N-S direction, while this decreases to 5 km near Aydın, 2.5 km near Sultanhisar. This situation might be related to the orientation of the BMDF. In the west, BMDF has located nearly 10 km in the north of the graben near Germencik. Towards the east of the graben, the detachment fault is very close to the graben floor (Figure 1b).

Based on mammal fossils contained in this unit, it was dated (Sarica, 2000; Ünay et al., 1995; Ünay & de Bruijn, 1998) to the latest Pliocene-Late Pleistocene age. Relict alluvial fans are divided into two subunits based on mammal fossil ages; the first one (Qraf1) consists of poorly sorted sandstone, mudstone, and marl. The deposits outcrop largely around Ortaklar and Aydın towns. The thick, coarse clastic rocks in the lower part of the succession were formed in a high-

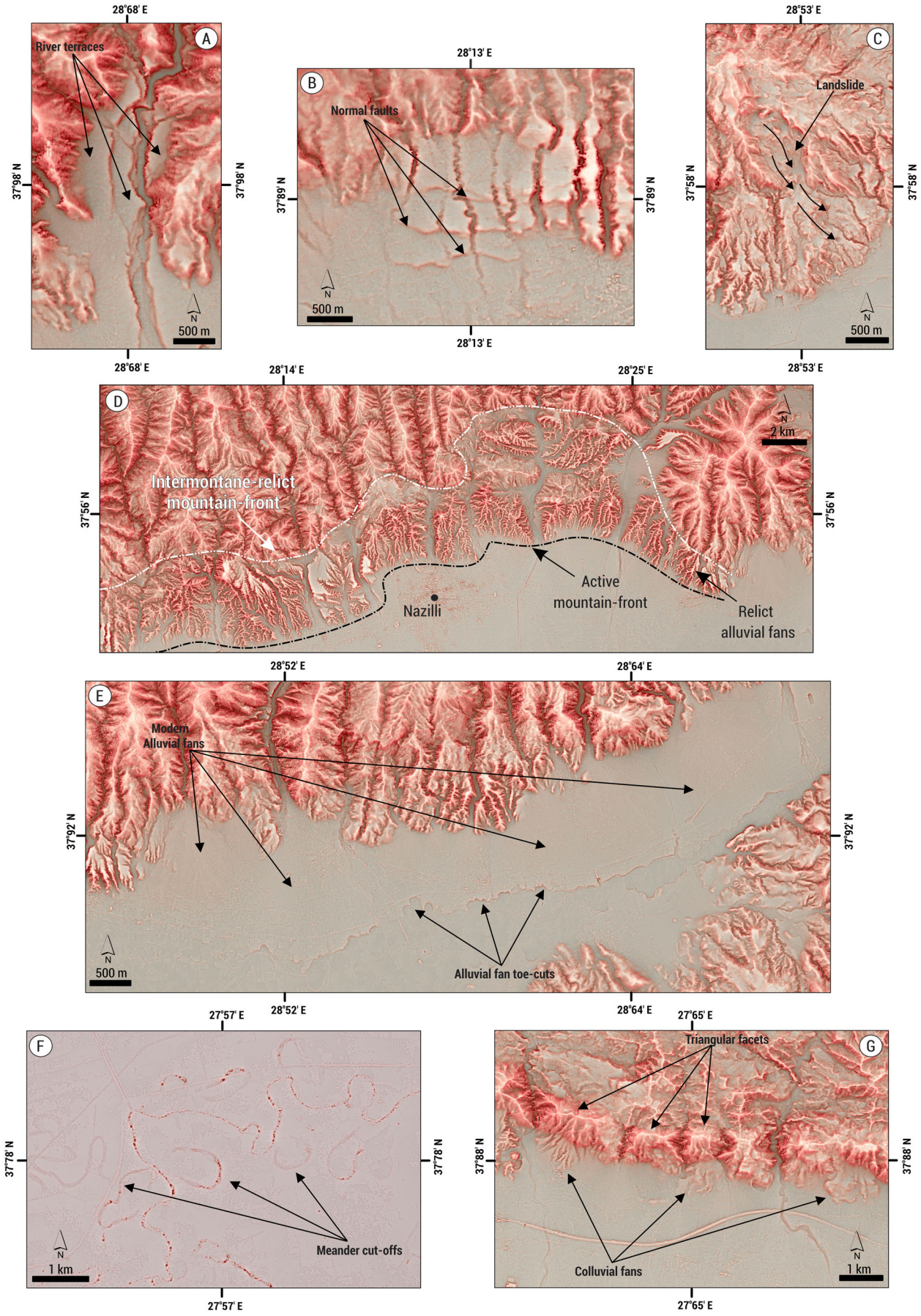

Figure 3. The examples of (a) the river terraces, (b) alluvial fan surface deformed by high-angle normal faults, (c) landslide, (d) relict alluvial fans, (e) modern alluvial fans and toe-cuts, (f) meander cut-offs and, (g) colluvial fans on the RRIM.

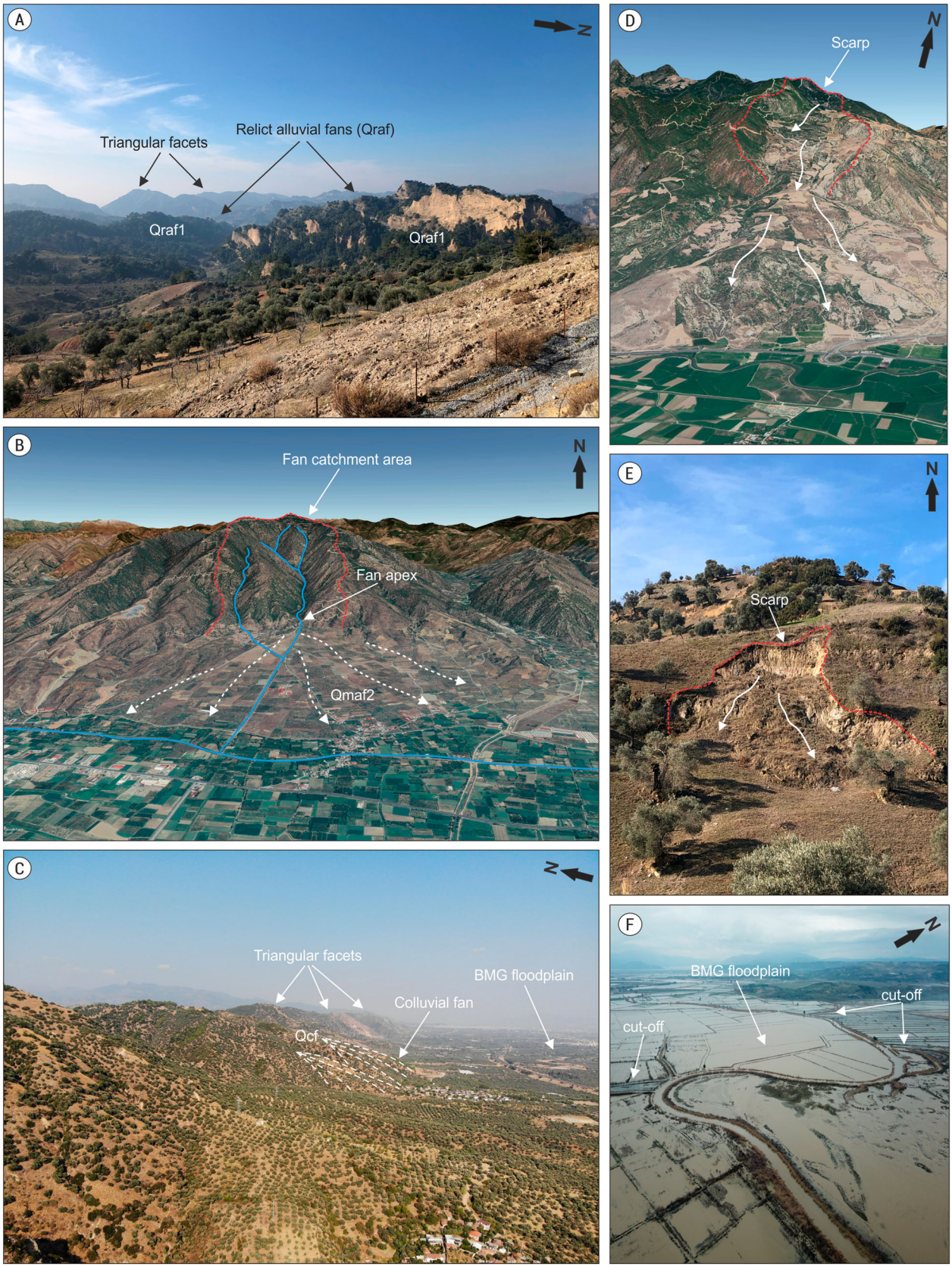

Figure 4. (a) The relict alluvial fans. (b) Modern alluvial fan in the eastern part of the BMG (Google Earth). (c) Colluvial fans and floodplain of the BMG. (d) Deep-seated landslide formed on Pliocene sediments (Google Earth). (e) Shallow landslide formed on relict alluvial fans. (f) Oblique drone picture of the cut-offs and the floodplain during a flood.

energy depositional environment. The oldest sediments (Qraf1), the deposition of which was related to the opening of the graben, are continuously exposed along the active northern margin (Gürer et al., 2009; Hakyemez et al., 1999). The second (Qraf2) is mainly poorly sorted, poorly bedded conglomerate, sandstone, and siltstone. The subunit may be younger than 0.4 Ma and older than the present-day graben floodplain

deposits (Gürer et al., 2009) (main map). The depositional characteristics of these sediments show an alluvial fan environment. The pebbles indicate imbrication fabric dipping N 8–30o, suggesting a provenance from the north and deposition by rivers. One of the important depositional characteristics of the relict alluvial fans is also back-tilting by the high-angle normal fault toward the north at varying angles. Especially around Aydın, back-tilting of sediments disrupts the original morphology of relict fans. The Tabakhane River deeply incised into relict alluvial fans as a response to back-tilting and uplift (Figure 5a and Figure 6c).

4.2. Modern alluvial fans (Qmaf)

There is no absolute age data on alluvial fans in the study area. We employed standard geomorphic principles such as elevation, weathering, soil thickness, surface dissection, and roughness (adopted from McFadden et al., 1989) of the fans to establish the morphostratigraphy of the alluvial fans.

The most voluminous alluvial fans developed along the northern mountain front of the BMG. The size, volume, and area of the alluvial fans change along the northern border of the BMG. While the surface area of the alluvial fans in the west section of the graben is larger, alluvial fans in the east section have a smaller area. The largest alluvial fan has an approximate surface of 48.5 km^2 and the smallest fan has an approximate surface of 260 m^2. The inclination of alluvial fan surfaces is very low (nearly 3%) in the west and middle section, on the contrary, they are higher (nearly 11%) in the eastern part (Figure 4b). Due to the high inclination of fans, alluvial fans in the east of the BMG are represented by nearly a 15% convex topographic gradient on the RRIM (Figure 3e). Catchment areas generally have an up to four times larger surface area compared to their corresponding alluvial fans in the west and middle part. However, catchment areas of the alluvial fans in the east section are smaller. While the alluvial fans in the east of the graben were deeply incised by rivers with depths of over 15 m, channels become wider and shallower, with depths varying from 1 to 4 m in the central part. In contrast, rivers form braided channel systems in the west section and they flow on the fan surface. Several toe-cuts are observed in the distal fan part toward the eastern part of the graben (Figure 3e). These toe cuts are formed by lateral erosion of the axial BMR rather than by vertical incision and base-level change in the main river. Also, several studies (Leeder & Mack, 2001; Larson et al., 2015; Giles et al., 2018) in the Basin and Range extensional region (USA) have shown that toe-cuts are an important indicator of high tectonic activity. The smaller alluvial fans are observed at the south margin of the BMG. The surface area of the largest alluvial fan is approximately 4.5 km^2. The catchment sizes of the alluvial fans are smaller in comparison to the northern alluvial fans (main map).

Modern alluvial fans are coarsely formed by metamorphic and granitic blocks. The sedimentological features of the modern alluvial fans show different texture and structure both to their position on the fan and toward the east of the BMG. During fieldwork, we observed that the apex part of the fans is characterized by poorly sorted, clast-supported, very angular, with large gravels and blocks up to 1–1.5 m in size. In the middle part of the fans, sediments are composed of moderately sorted, angular and sub-angular, clast-supported, coarse sands, and gravels. Toward the fan-toe, sediments are characterized by sub-rounded, well-sorted clasts, fine-grained sand, and clast-supported gravels. In addition, in the west and middle sections of the BMG, alluvial fans are represented by more consolidated, well-sorted, sub-rounded clasts, with sand, gravels, and pebbles. In contrast, fans in the east section show unconsolidated, poorly sorted, very angular, with large gravels and blocks (Figure 6e,f).

Along the strike of the BMG, the relative age of alluvial fans showing different development features is thought to be different. The degree of weathering and soil thickness on the alluvial fans are higher in the west and middle sections. A dense river network developed on fan systems in these sections. Nevertheless, in the eastern section soil thickness, weathering, and the fluvial network are more weakly developed. In the general sense, the alluvial fans are relatively getting younger toward the east of the BMG. The modern alluvial fans were mapped as Qmaf1 starting from the westernmost of the BMG up to the Kuyucak town. As from the Kuyucak, alluvial fans were defined as Qmaf2 based on relationships with relative ages. Several alluvial fans have developed on the older alluvial fans between the Sultanhisar and the Kuyucak town. We observed that the younger sediments prograde distally to form a generally telescopic-like alluvial fan structure (main map).

The Çine graben is a half-graben in the west of the study area. A Quaternary normal fault bounds the east of the graben. The alluvial fans are mostly observed on the east side of the graben. In the eastern section, Qmaf1 fan surfaces are deeply incised by the rivers. Relatively smaller size alluvial fans are developed in the southwestern of the graben defined as Qmaf2. The Bozdoğan half-graben is in the center of two other half-grabens. The western mountain front of the graben is delimited by a normal fault. In this section, the alluvial fan volumes and areas are larger in comparison to the eastern mountain front of the graben. All alluvial fans of this graben were defined as Qmaf2 based on their similar weathering, soil thickness, and surface roughness. The NW-SE striking Karacasu half-graben is located further east. Compared to other half-grabens, alluvial fans developed intensely on

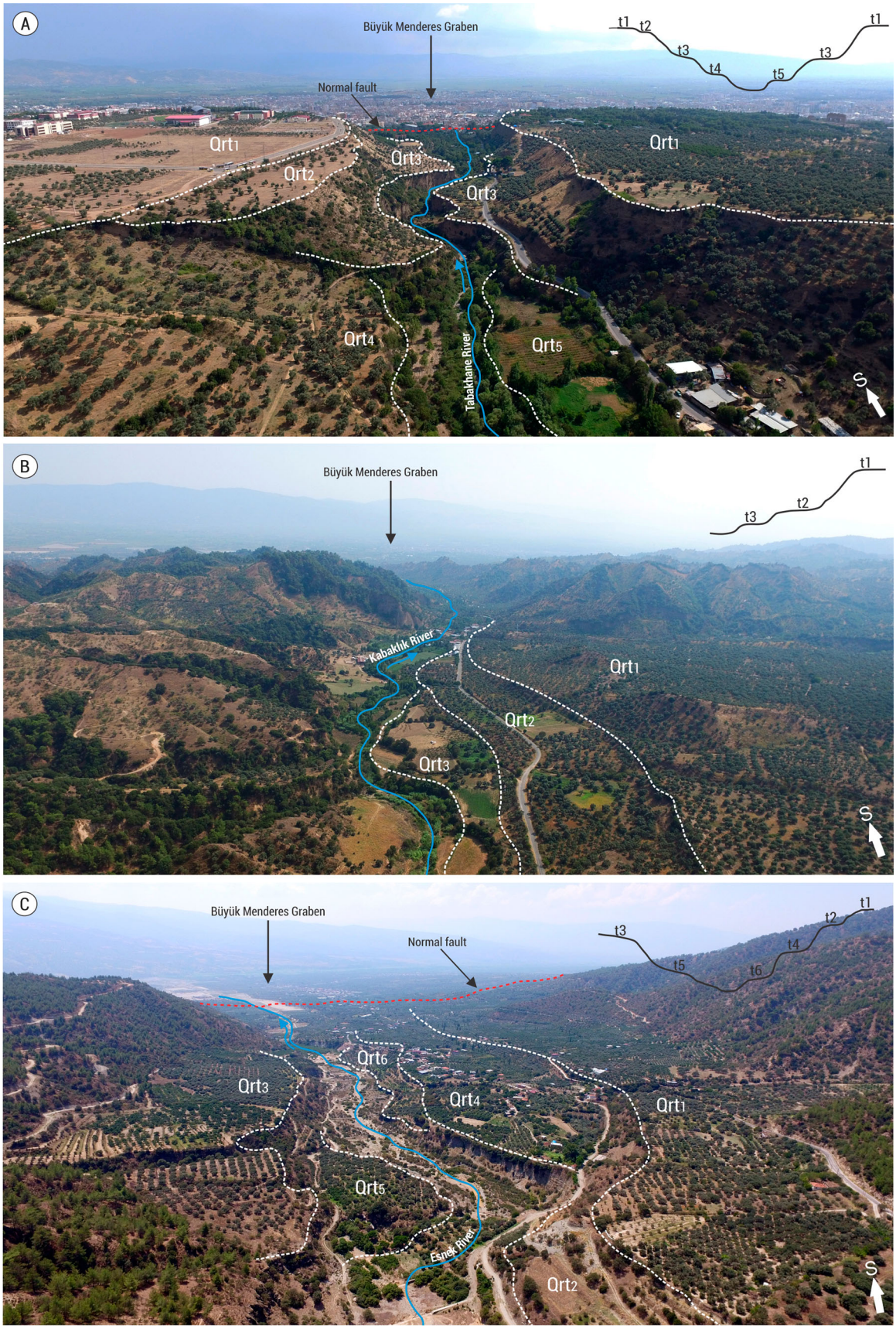

Figure 5. Oblique drone pictures of the river terraces. (a) Tabakhane, (b) Kabaklık, and (c) Esnek River. See Figure 1c for locations.

the western mountain front of the graben. The western margin of the graben is also controlled by normal faults. The volumes and thicknesses of alluvial fans at this margin are greater and are deeply incised by rivers. Alluvial fans along the eastern mountain front of the graben are only observed in the southeast. Sediments of the alluvial fans in this part are represented by unconsolidated, poorly sorted with angular gravels

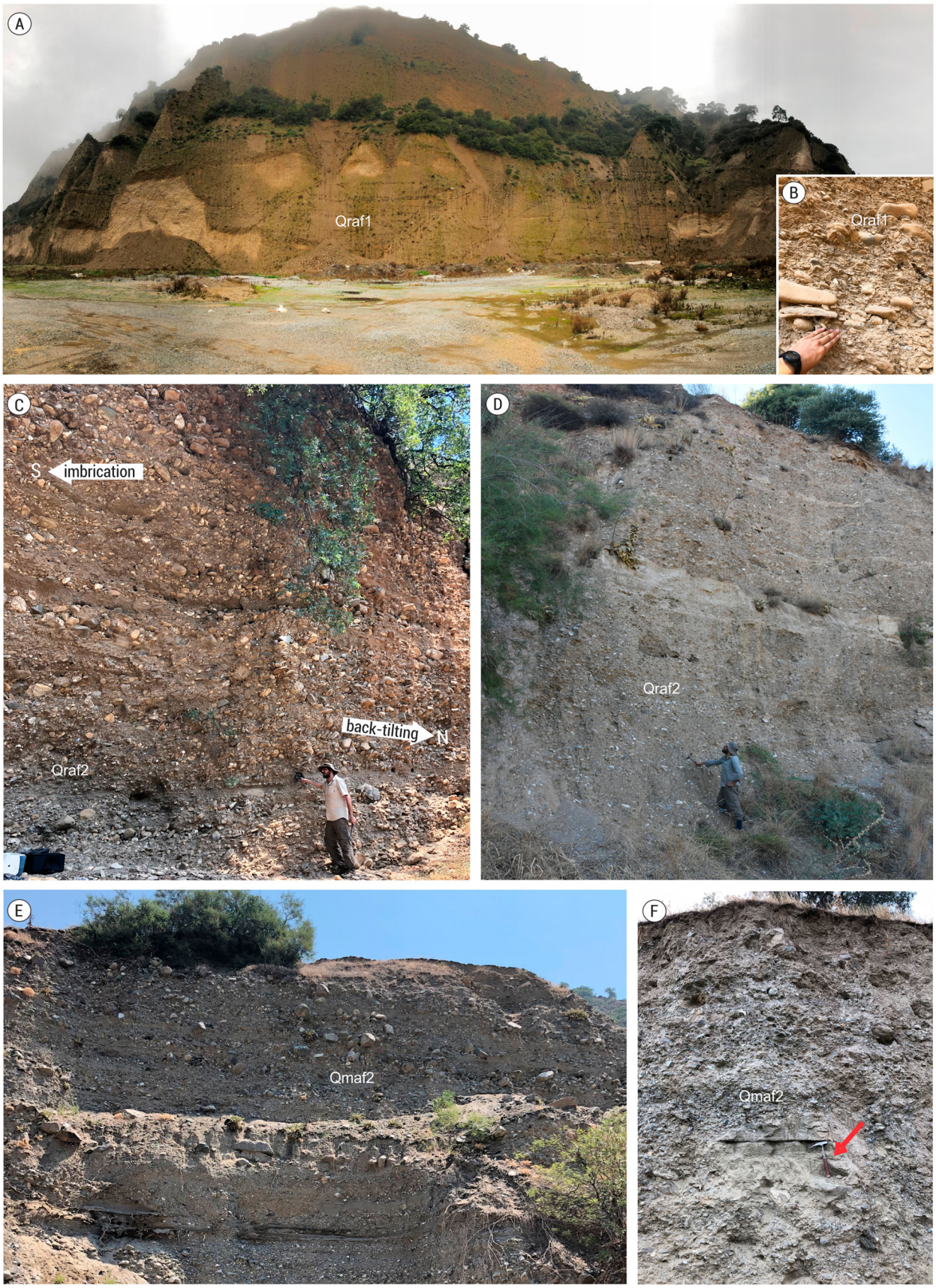

Figure 6. Deposits of the relict and modern alluvial fans. (a) The relict alluvial fan deposits named the *Tmolosschutt*. (b) The poorly sorted sediment structure of the relict alluvial fans. (c) The sediments of the relict alluvial fan back-tilted to the north. (d) A view of the more unconsolidated sediments toward the surface of the relict alluvial fans. (e,f) Sedimentary body of a modern alluvial fan with unconsolidated, angular, and poorly sorted clasts, in the eastern section of the BMG. The geological hammer is marked with a red arrow.

and blocks. In contrast to the western mountain front, river networks, soil, and vegetation are weakly developed on the fans. Due to the above features, we mapped as Qmaf2 the alluvial fans in this section. The development of alluvial fans in this graben was more complex compared to the other two half-grabens. Some drill core data were presented by Alçiçek and Jiménez-Moreno (2013) on the graben and it was revealed that these units were of Quaternary age (main map).

4.3. River terraces (Qrt)

The river terraces were identified at different levels along the southern flank of the Aydın Mountain. These river terraces are on the footwall block of the by high-angle normal faults (Figure 1c). The rivers on the Aydın Mountain flow into the BMG. The BMG forming the hanging-wall block is a base level for rivers flowing south from the Aydın Block. Well-developed river terraces within a staircase can be linked to increased rates of base-level change (e.g. tectonic uplift) (Mather et al., 2017; Meikle et al., 2010). The river terraces in extensional regions were used to explain the role of the faulting, regional uplift, and base level change (Maddy et al., 2020; Ocakoğlu, 2020). Accordingly, the river terraces in the study area are important archives recording tectonic movements and base-level changes in the region.

All river terrace surfaces show high positive openness values because of their flat surfaces. Terraces surfaces were clearly distinguishable on the RRIM (Figure 3a). The Tabakhane Basin is located in the north of the Aydın city. The river flows through the relict and modern fans and in the confluence at the BMR. The length of the river is about 25 km from the peak of the Aydın Mountain to BMR. We determined five terrace levels with elevations of 90 ± 0.2 m, 85 ± 0.2 m, 32 ± 0.2 m, 20 ± 0.2 m, and 5 ± 0.2 m above the Tabakhane River. In the west of the river, four terrace levels were observed, while the east two terrace levels were exposed. The Tabakhane River terraces formed resulting in the deep incision of its course on deposits of the relict alluvial fans. We did not observe any strath terraces belonging to Tabakhane River. From the bottom of the valley toward the highest terrace surface, sediments are characterized by more unconsolidated gravel. One of the most important features of the sediments is that the imbrication of conglomerates is toward the south. However, these conglomerates and large blocks are tilted about 20° toward the north. Gürer et al. (2009) stated that high-angle normal faults extending along the mountain front tilted the relict alluvial fan deposits toward the north (Figure 5a, Figure 6c and main map 1).

The Kabaklık Basin is located in the northwest of Köşk town. The total length of the Kabaklık River is about 17 km from spring to where the river is joined to BMR. The three-terrace staircase is defined with elevations of 55 ± 0.2 m, 18 ± 0.2 m, and 6 ± 0.2 m above the Kabaklık River. Though fluvial terraces are exposed west of the Kabaklık River, only levels of the T2 terrace are exposed. These terraces formed on relict alluvial fan deposits. Accordingly, sediments show similar characteristics. Any strath terraces belonging to the Kabaklık River were also not observed. Similarly, the sediments showing the imbrication of conglomerates toward the south are tilted about 12° toward the north (Figure 5b and main map 1).

The Esnek Basin located in the east has the best-preserved fluvial terraces. The total length of the Esnek River is 23 km. The river incised deeply its course in the apex part of the fan with 92 m. The six-terrace levels have elevations of 92 ± 0.2 m, 70 ± 0.2 m, 46 ± 0.2 m, 35 ± 0.2 m, 22 ± 0.2 m, and 15 ± 0.2 m above the Esnek River. The four different terraces outcrop west of the Esnek River, while two different terraces are observed in the east. The Esnek river terraces formed on the modern alluvial fan. There are no strath terrace deposits of the river on the terrace surface. From the modern course of the river toward the Qrt1 terrace surface, sediments comprise more unconsolidated and finer grain sizes. The imbrication of clasts in the sediments is to the south. In contrast to Tabakhane and Kabaklık, the tilting on the sediments belonging to the Esnek River terraces were not observed (Figure 5c and main map 2).

4.4. Colluvial fans (Qcf)

Colluvial fans are represented by the medium white color due to their convex topography on RRIM (Figure 3g). Colluvial fans are generally observed between İncirliova and Germencik town in the west of the BMG (Figure 3f and Figure 4c). The İncirliova Fault segment striking E-W is a border between the colluvial fans and the triangular facets formed from the metamorphic rocks. The majority of the sediments are deposited directly on the graben and are separated with a clast-supported, poorly sorted, very angular cobbles and blocks displaying a chaotic deposition environment in comparison with relict and modern alluvial fans. While alluvial fan sediments show imbrication toward BMG, the colluvial fan sediments do not show any imbrication features. The colluvial fans show a high inclination (nearly 14%) compared to alluvial fans.

4.5. Floodplain (Qfp) and meander cut-offs (Qmc)

Etymologically the term ‘meander’ comes from the Menderes River (*Maiandros flu* in Greek) (Kazancı et al., 2011) because of every kind of meander related form along the floodplain of the valley. On the

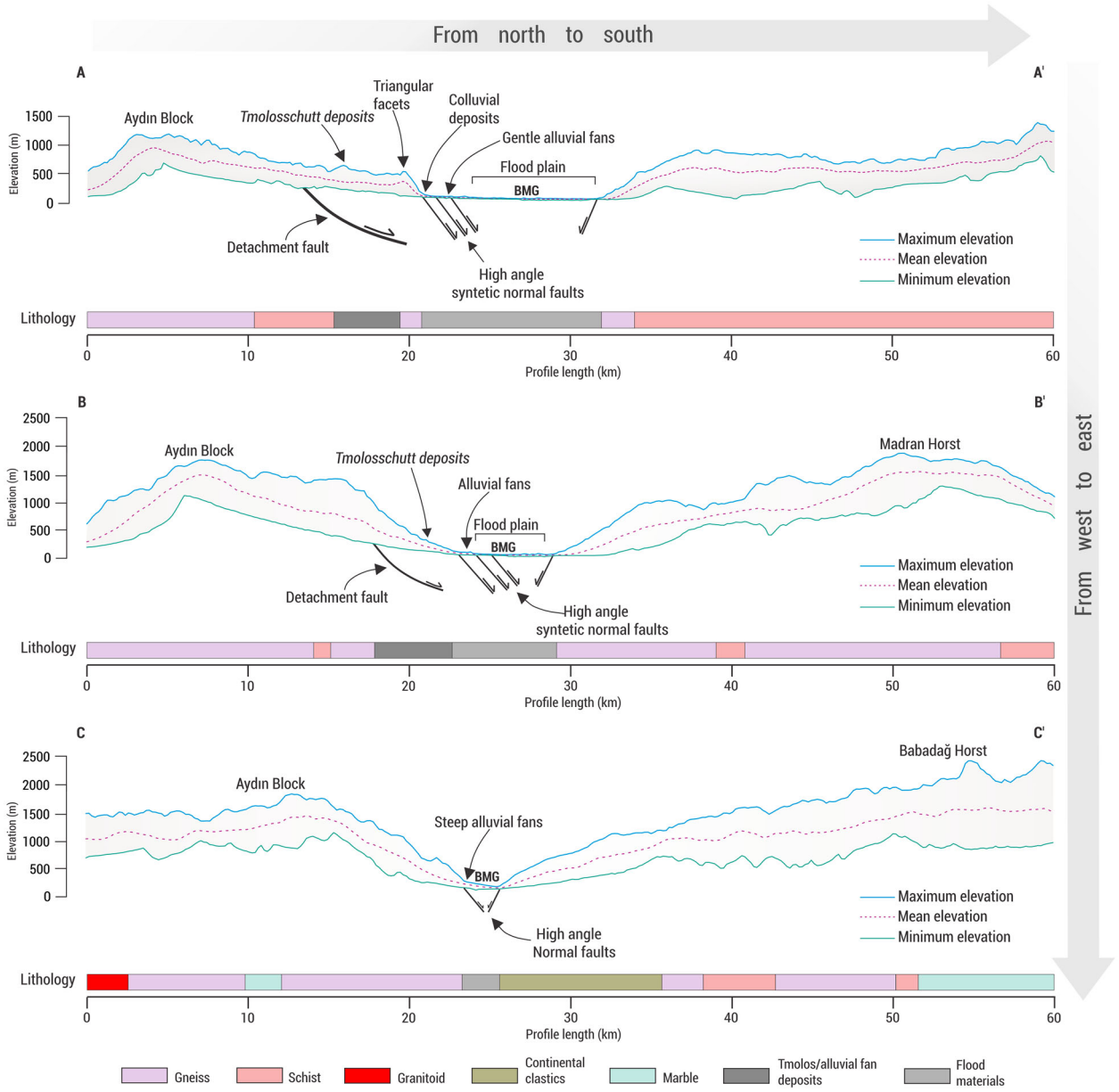

Figure 7. Swath profiles from west to the east. See Figure 1c for the locality of the swath sections.

floodplain of the BMG, the basic units are abandoned channels, cut-offs, ox-bow lakes, ponds, point bars, and active meandering channels of the BMR. With nearly 543 km length and 50 m width within the graben, the river is one of Turkey's major rivers. In the central and especially in the western sections of the graben, alluvial fans propagating to the south give rise to the southward migration of the main course of the BMR. Meander cut-offs are mostly observed in the west section of the BMG (Figure 3f and main map 1). The formation period for the cut-offs is associated with floods occurring on the BMR. During floods, fast flow by the BMR caused it to abandon these meander bends (Figure 4f). The old cut-offs were filled over time by sedimentation processes; however, current cut-offs are mostly in the form of oxbow lakes. In the central and east sections of the graben, cut-offs are considered to be covered by active alluvial fans.

4.6. Landslides (Ql)

The spatial distribution of landslides was extracted from the General Directorate of Mineral Research and Exploration (MTA) portal (Duman et al., 2011), and most landslides were confirmed during fieldwork. Görüm (2019) showed that landslides can clearly be recognized from the RRIM. While the scarps of the landslides show high negative openness values due to slope, positive openness values increase toward their accumulation zone (Figure 3c). Landslides are observed in the west and east of the graben. Landslides occurring in the east section of the Aydın Mountain have deeper characteristics (depth of sliding surface > 5 m) (Figure 4d). In the west, landslides intensify on relict alluvial fan sediments. In this section, the relief is very low (Figure 7) and most landslides have shallow characteristics (depth of sliding surface < 5 m) (Figure 4e).

4.7. Coastal dunes (Qcd), swamps (Qs) and paleo-shorelines (Qps)

The three shallow lagoons are observed on the Büyük Menderes Delta (BMD). The lagoons have been separated from the sea by narrow coastal spits. Coastal dunes behind the lagoons have been formed by the accumulation of sand transported by westerly winds with the reduction of soil humidity in the summer period. The main source of the dunes consists of sediments transported by the BMR. Swamps are located between the lagoons and the dunes. These swamps dry in the summer period, and become swamps again in winter and especially in flood periods.

Geoarchaeological investigations (Brückner, 2005; Brückner et al., 2017; Eisma, 1978; Erinc, 1978) attest to the historical shorelines and the rapid progradation of the Büyük Menderes Delta, especially since the 1st millennium BC. We prefer to present the seven historical shorelines of the delta on the main map based on Brückner et al. (2017) which is the most comprehensive study. The shorelines are very important to understand the relationship between the disappearance of the ancient sites and delta progradation. The Mid-Holocene erosion in the southern section of the Menderes Massif is responsible for one of the greatest sediment redistributions in Turkey and further caused rapid alluvial filling of ancient harbor cities such as Miletus, Myous and Priene which are 40 km away from the modern coastline (main map 1).

5. Discussion and conclusion

We identified ten different Quaternary landforms on the main map. The most common landforms are relict and modern alluvial fans, river terraces, and floodplains. One of the important components in understanding the evolution of the landscape is building a morphostratigraphy of landforms. Although we do not have absolute ages of landforms we can have a tentative interpretation. The oldest depositional landforms are relict alluvial fans represents the early stage of the BMGS that is driven by exhumation of the Menderes Massif along detachment faults. Today, this first generation (relict alluvial fans) is strongly deformed (e.g. faulted, uplifted, tilted) and has lost its original fan geometry. Deformation of the relict fans away from the detachment fault indicates the growth of younger faults and basinward migration of deformation. Protracted extension of the graben provides more accommodation space to develop modern alluvial fans to incise the relict alluvial fans. These modern fans were also faulted and deformed at some places but they still preserve their alluvial fan shape. The presence of river terraces within alluvial fans indicates abandonment of the modern alluvial fans and starting of the third stage of landscape evolution. The non-uniform distribution of river terraces indicates the effect of local faulting on their development. These terraces were incised and the last stage of evolution started. The last stage is the infilling of graben floors by intensive alluvial sedimentation on floodplains. This is because of Holocene sea level transgression along the graben. The presence of paleo-shorelines aligned along the flood plain indicates propagation of the graben floodplain towards the Aegean Sea and the formation of the modern Büyük Menderes Graben in the late Holocene.

The spatial pattern of the alluvial fans and river terraces implies variable rates of tectonics and surface processes along the strike of the graben system. The size, volume, and area of the alluvial fans change along the northern border of the BMG. This situation may be explained by differential tectonic activity along the northern mountain front of the BMG. Also, the size of the drainage basins and alluvial fans along the southern mountain front of the BMG are relatively smaller than their counterparts along the northern mountain fronts. We believe that this is also a geomorphic marker indicating relatively less vertical displacement along the southern mountain front which has not produced sufficient uplift to provide material for drainage basins to support large alluvial fans. The main map shows that Çine, Karacasu, and Bozdoğan grabens have different morphostratigraphic units than the BMG. The Büyük Menderes River is the local base level for these half-graben drainage systems, but morphostratigraphical differences among these secondary grabens imply the activity of faults within their basin.

The presence of many propagating paleo-shorelines (main map) reveals rapid alluvial filling downstream of the graben and also high erosion rates at the upstream reaches of the Büyük Menderes Graben. The random distribution of abandoned channels and meander cut-offs indicates the high potential of the flood hazard along the main river in the west part of the BMG. Floodplains along the trunk and tributary rivers are rich in terms of alluvial landforms associated with meandering channel patterns. These areas are also prone to geohazards such as floods and liquefaction. Also, many landslides in the west and the east along the southern mountain-front of the Aydın Mountain are observed. Landslides in the region may pose problems for agriculture areas and settlements. In this context, this study contributes to the understanding of the Quaternary landscape evolution of Southern Menderes Massif and provides a basis for future geological and natural hazard studies in the region.

Acknowledgments

This paper is a part of the first author's Ph.D. thesis. The first author thanks The Scientific and Technological Research

Council of Turkey (TÜBİTAK), International Research Fellowship Programme for Ph.D. students (BİDEB 2214-A). We also thank Associate Editor J. Knight and reviewers M. Stokes, M. Shand, and M. Gul for their constructive comments that significantly improved the manuscript.

Software

The digitizing of landforms and in the preparation of this map were performed with ESRI ArcMap 10.6. Red Relief Image Map was produced with SAGA GIS. The final editing was carried out with the ADOBE Illustrator CS6.

Disclosure statement

No potential conflict of interest was reported by the author(s).

Funding

This study was funded by The Scientific and Technological Research Council of Turkey [grant number 116Y077] and Istanbul Technical University [grant number TDK-2019-41838].

ORCID

Emrah Özpolat http://orcid.org/0000-0002-1829-0152
Cengiz Yıldırım http://orcid.org/0000-0001-5253-028X
Tolga Görüm http://orcid.org/0000-0001-9407-7946

References

Aktug, B., Nocquet, J. M., Cingöz, A., Parsons, B., Erkan, Y., England, P., Lenk, O., Gürdal, M. A., Kilicoglu, A., Akdeniz, H., & Tekgül, A. (2009). Deformation of western Turkey from a combination of permanent and campaign GPS data: Limits to block-like behavior. *Journal of Geophysical Research*, *114*(B10404). https://doi.org/10.1029/2008JB006000

Alçiçek, H., & Jiménez-Moreno, G. (2013). Late Miocene to Plio-Pleistocene fluvio-lacustrine system in the Karacasu Basin (SW Anatolia, Turkey): Depositional, paleogeographic and paleoclimatic implications. *Sedimentary Geology*, *291*, 62–83. https://doi.org/10.1016/j.sedgeo.2013.03.014

Altunel, E. (1998). Evidence for Damaging Historical Earthquakes at Priene, Western Turkey. *Turkish Journal of Earth Sciences*, *7*(1), 25–36.

Anthony, E. J., Marriner, N., & Morhange, C. (2014). Human influence and the changing geomorphology of Mediterranean deltas and coasts over the last 6000 years: From progradation to destruction phase? *Earth Science Reviews*, *139*, 336–361. https://doi.org/10.1016/j.earscirev.2014.10.003

Armijo, R., Meyer, B., Hubert, A., & Barka, A. (1999). Westward propagation of the North Anatolian fault into the northern Aegean: Timing and kinematics. *Geology*, *27*(3), 267–270. https://doi.org/10.1130/0091-7613(1999)027<0267:WPOTNA>2.3.CO;2

Barka, A., & Reilinger, R. (1997). Active tectonics of the Eastern Mediterranean region: Deduced from GPS, neotectonic and seismicity data. *Annali Di Geofisica*. https://doi.org/10.4401/ag-3892

Bertotti, G., Capozzi, R., & Picotti, V. (1997). Extension controls Quaternary tectonics, geomorphology and sedimentation of the N-Appennies foothills and adjacent Po Plain (Italy). *Tectonophysics*, *282*(1-4), 291–301. https://doi.org/10.1016/S0040-1951(97)00229-1

Blair, T. C. (1999). Sedimentology of the debris-flow-dominated Warm Spring Canyon alluvial fan, Death Valley, California. *Sedimentology*, *46*(5), 941–965. https://doi.org/10.1046/j.1365-3091.1999.00260.x

Boulton, S. J., & Stokes, M. (2018). Which DEM is best for analyzing fluvial landscape development in mountainous terrains? *Geomorphology*, *310*, 168–187. https://doi.org/10.1016/j.geomorph.2018.03.002

Bozkurt, E. (2000). Timing of extension on the büyük Menderes Graben, Western Turkey and its tectonic implications. In E. Bozkurt, J. A. Winchester, & J. D. A. Piper (Eds.), *Tectonics and Magmatism in Turkey and the surrounding area* (pp. 385–403). Geological Society, Special Publications 173.

Brückner, H. (1997). Coastal changes in western Turkey; rapid delta progradation in historical times. *Bulletin de l'Institut Océanographique*, *18*, 63–74.

Brückner, H. (2005). Holocene shoreline displacements and their consequences for human societies: The example of Ephesus in western Turkey. *Zeitschrift fur Geomorphologie*, *137*(Suppl.), 11–22.

Brückner, H., Herda, A., Kerschner, M., Müllenhoff, M., & Stock, F. (2017). Life cycle of estuarine islands—from the formation to the landlocking of former islands in the environs of Miletos and Ephesos in western Asia Minor (Turkey). *Journal of Archaeological Science: Reports*, *12*, 876–894. https://doi.org/10.1016/j.jasrep.2016.11.024

Chiba, T., Kaneta, S.-I., & Suzuki, Y. (2008). Red relief image map: New visualization method for three dimensional data. *The International Archives of the Photogrammetry, Remote Sensing and Spatial Information Sciences*, *37*(B2), 1071–1076. https://doi.org/10.11212/jjca1963.45.27

Cohen, H. A., Dart, C. J., Akyuz, H. S., & Barka, A. (1995). Syn-rift sedimentation and structural development of the Gediz and Buyuk Menderes Graben, western Turkey. *Journal-Geological Society (London)*, *152*(4), 629–638. https://doi.org/10.1144/gsjgs.152.4.0629

Dewey, J. F., & Şengör, A.C. (1979). Aegean and surrounding regions: Complex multiplate and continuum tectonics in a convergent zone. *Geological Society of America Bulletin*, *90*(1), 84-92. https://doi.org/10.1130/0016-7606(1979)90<84:AASRCM>2.0.CO;2

DLR. (2016). TanDEM-X ground segment DEM products specification document TD-GS-PS-0021 v.3.1. DLR. (46 pp).

Duman, T. Y., Çan, T., & Emre, Ö. (2011). '1:1,500,000 scale landslide inventory map of Turkey. General directorate of mineral research and exploration, special publication series-27. Ankara-Turkey.

Eisma, D. (1978). Stream deposition and erosion by the eastern shore of the Aegean. In W. C. Brice (Ed.), *The environmental history of the near and middle east since the lastice age* (pp. 67–81). Academic Press.

Emre, Ö, Duman, T. Y., Özalp, S., Şaroğlu, F., Olgun, Ş, Elmacı, H., & Can, T. (2018). Active fault database of Turkey. *Bulletin of Earthquake Engineering*, *16*(8), 3229–3275. https://doi.org/10.1007/s10518-016-0041-2

Ergin, M., Kadir, S., Keskin, Ş, Turhan-Akyüz, N., & Yaşar, D. (2007). Late quaternary climate and sea-level changes

recorded in sediment composition off the Büyük Menderes River delta (eastern Aegean Sea, Turkey). *Quaternary International*, *167-168*, 162–176. https://doi.org/10.1016/j.quaint.2007.02.009

Erinc, S. (1978). Changes in the physical environment in Turkey since the end of the last glacial. In W. C. Brice (Ed.), *The environmental history of the near and middle east since the last ice age* (pp. 87–110). Academic Press.

Erinç, S. (1954). Über die Entstehung und morphologische Bedeutung des Tmolosschutts. *Review of the Geographical Institute of the University of Istanbul*, *2*, 55–72.

Fountoulis, I., Vassilakis, E., Mavroulis, S., Alexopoulos, J., Dilalos, S., & Erkeki, A. (2015). Synergy of tectonic geomorphology, applied geophysics and remote sensing techniques reveals new data for active extensional tectonism in NW Peloponnese (Greece). *Geomorphology*, *237*, 52–64. https://doi.org/10.1016/j.geomorph.2014.11.016

Gessner, K., Gallardo, L. A., Markwitz, V., Ring, U., & Thomson, S. N. (2013). What caused the denudation of the Menderes Massif: Review of crustal evolution, lithosphere structure, and dynamic topography in southwest Turkey. *Gondwana Research*, *24*(1), 243–274. https://doi.org/10.1016/j.gr.2013.01.005

Giles, P. T., Whitehouse, B. M., & Karymbalis, E. (2018). Interactions between alluvial fans and axial rivers in Yukon, Canada and Alaska, USA. *Geological Society, London, Special Publications*, *440*(1), 23–43. http://doi.org/10.1144/SP440.3

Görüm, T. (2019). Landslide recognition and mapping in a mixed forest environment from airborne LiDAR data. *Engineering Geology*, *258*, 105155. https://doi.org/10.1016/j.enggeo.2019.105155

Gürer, Ö. F., Sarica-Filoreau, N., Özburan, M., Sangu, E., & Doğan, B. (2009). Progressive development of the büyük Menderes Graben based on new data, western Turkey. *Geological Magazine*, *146*(5), 652–673. https://doi.org/10.1017/S0016756809006359

Hakyemez, H. Y., Erkal, T., & Göktas, F. (1999). Late Quaternary evolution of the Gediz and Buyuk Menderes grabens, western Anatolia, Turkey. *Quaternary Science Reviews*, *18*(4–5), 549–554. https://doi.org/10.1016/S0277-3791(98)00096-1

Kazanci, N., Dündar, S., Alçiçek, M. C., & Gürbüz, A. (2009). Quaternary deposits of the Büyük Menderes Graben in western Anatolia, Turkey: Implications for river capture and the longest Holocene estuary in the Aegean Sea. *Marine Geology*, *264*(3–4), 165–176. https://doi.org/10.1016/j.margeo.2009.05.003

Kazancı, N., Gürbüz, A., & Boyraz, S. (2011). Büyük Menderes nehri'nin jeolojisi ve evrimi. *Türkiye Jeoloji Bülteni*, *54*(12), 25–56.

Konak, N., & Şenel, M. (2002). Geological map of Turkey in 1/500.000 scale: Denizli sheet. *Publication of Mineral Research and Exploration Directorate of Turkey (MTA), Ankara*.

Larson, P. H., Dorn, R. I., Faulkner, D. J., & Friend, D. A. (2015). Toe-cut terraces: A review and proposed criteria to differentiate from traditional fluvial terraces. *Progress in Physical Geography*, *39*(4), 417–439. https://doi.org/10.1177/0309133315582045

Leeder, M. R., & Mack, G. H. (2001). Lateral erosion ('toe-cutting') of alluvial fans by axial rivers: Implications for basin analysis and architecture. *Journal of the Geological Society*, *158*(6), 885–893. https://doi.org/10.1144/0016-760000-198

Maddy, D., Veldkamp, A., Demir, T., Aytaç, A. S., Schoorl, J. M., Scaife, R., Boomer, I., Stemerdink, C., Van Der Schriek, T., Aksay, S., & Lievens, C. (2020). Early Pleistocene River Terraces of the Gediz River, Turkey: The role of faulting, fracturing, volcanism and travertines in their genesis. *Geomorphology*, *358*, 107102. https://doi.org/10.1016/j.geomorph.2020.107102

Mather, A. E., Stokes, M., & Whitfield, E. (2017). River terraces and alluvial fans: The case for an integrated Quaternary fluvial archive. *Quaternary Science Reviews*, *166*, 74–90. https://doi.org/10.1016/j.quascirev.2016.09.022

McFadden, L. D., Ritter, J. B., & Wells, S. G. (1989). Use of multiparameter relative-age methods for age estimation and correlation of alluvial fan surfaces on a desert piedmont, eastern Mojave Desert, California. *Quaternary Research*, *32*(3), 276–290. https://doi.org/10.1016/0033-5894(89)90094-X

Meikle, C., Stokes, M., & Maddy, D. (2010). Field mapping and GIS visualisation of Quaternary river terrace landforms: An example from the Rio Almanzora, SE Spain. *Journal of Maps*, *6*(1), 531–542. https://doi.org/10.4113/jom.2010.1100

Mozafari, N. (2019). Holocene seismic activity of the Priene-Sazlı Fault revealed by cosmogenic 36Cl, Western Anatolia, Turkey. *Turkish Journal of Earth Sciences*. https://doi.org/10.3906/yer-1810-6

Ocakoğlu, F. (2020). Rapid Late Quaternary denudation of the Karacasu Graben in response to subsidence in the Büyük Menderes Corridor: Insights from morphotectonics and archaeogeology. *Geomorphology*, *107107*. https://doi.org/10.1016/j.geomorph.2020.107107

Ocakoğlu, F., Açikalin, S., Özsayin, E., & Dirik, R. K. (2014). Tectonosedimentary evolution of the Karacasu and Bozdoğan basins in the central Menderes Massif, W Anatolia. *Turkish Journal of Earth Sciences*, *23*(4), 361–385. https://doi.org/10.3906/yer-1309-12

Oner, Z., & Dilek, Y. (2011). Supradetachment basin evolution during continental extension: The Aegean province of western Anatolia. *Turkey. Bulletin*, *123*(11-12), 2115–2141. https://doi.org/10.1130/B30468.1

Philippson, A. (1912). *Reisen und Forschungen im westlichen Kleinasien (No. 1-5)*. Justus Perthes.

Reilinger, R., McClusky, S., Vernant, P., Lawrence, S., Ergintav, S., Cakmak, R., Ozener, H., Kadirov, F., Guliev, I., Stepanyan, R., & Nadariya, M. (2006). GPS constraints on continental deformation in the Africa-Arabia-eurasia continental collision zone and implications for the dynamics of plate interactions. *Journal of Geophysical Research: Solid Earth*, *111*, B5. https://doi.org/10.1029/2005JB004051

Sarica, N. (2000). The Plio-Pleistocene age of Büyük Menderes and Gediz grabens and their tectonic significance on N-S extensional tectonics in West Anatolia: Mammalian evidence from the continental deposits. *Geological Journal*, *35*(1), 1–24. https://doi.org/10.1002/(SICI)1099-1034(200001/03)35:1<1::AID-GJ834>3.0.CO;2-A

Şengör, A. C., & Yilmaz, Y. (1981). Tethyan evolution of Turkey: A plate tectonic approach. *Tectonophysics*, *75*(3-4), 181–241. https://doi.org/10.1016/0040-1951(81)90275-4

Sümer, Ö, İnci, U., & Sözbilir, H. (2013). Tectonic evolution of the Söke Basin: Extension-dominated transtensional basin formation in western part of the Büyük Menderes Graben, Western Anatolia, Turkey. *Journal of*

Geodynamics, *65*, 148–175. https://doi.org/10.1016/j.jog.2012.06.005

Tsodoulos, I. M., Koukouvelas, I. K., & Pavlides, S. (2008). Tectonic geomorphology of the easternmost extension of the Gulf of Corinth (Beotia, Central Greece). *Tectonophysics*, *453*(1-4), 211–232. https://doi.org/10.1016/j.tecto.2007.06.015

Ünay, E., & de Bruijn, H. (1998). Plio-Pleistocene rodents and lagomorphs from Anatolia. *Mededelingen Nederlands Instituut voor Toegepaste Geowetenschappen TNO*, *60*, 431–466.

Ünay, E., Göktaş, F., Hakyemez, H. Y., Avşar, M., & Şan, Ö. (1995). Dating the sediments exposed at the northern part of the büyük Menderes Graben (Turkey) on the basis of Arvicolidae (Rodentia, Mammalia). *Geological Bulletin of Turkey*, *38*(2), 63–68.

Valente, E., Buscher, J. T., Jourdan, F., Petrosino, P., Reddy, S. M., Tavani, S., Corradetti, A., & Ascione, A. (2019). Constraining mountain front tectonic activity in extensional setting from geomorphology and Quaternary stratigraphy: A case study from the Matese ridge, southern Apennines. *Quaternary Science Reviews*, *219*, 47–67. https://doi.org/10.1016/j.quascirev.2019.07.001

Wölfler, A., Glotzbach, C., Heineke, C., Nilius, N. P., Hetzel, R., Hampel, A., Akal, C., Dunkl, I., & Christl, M. (2017). Late Cenozoic cooling history of the central Menderes Massif: Timing of the Büyük Menderes detachment and the relative contribution of normal faulting and erosion to rock exhumation. *Tectonophysics*, *717*, 585–598. https://doi.org/10.1016/j.tecto.2017.07.004

Yokoyama, R., Shirasawa, M., & Pike, R. J. (2002). Visualizing topography by openness: A new application of image processing to digital elevation models. *Photogrammetric Engineering and Remote Sensing*, *68*(3), 257–266.

Yönlü, Ö, Altunel, E., Karabacak, V., Akyüz, S., & Yalçıner, Ç. (2010). Offset archaeological relics in the western part of the Büyük Menderes graben (western Turkey) and their tectonic implications. *Geological Society of America Special Paper*, *471*, 269–279. https://doi.org/10.1130/2010.2471(21)